Velocity analysis of converted waves based on hyperbolic moveout equation

Vladimir Grechka and Ilya Tsvankin
Center for Wave Phenomena, Department of Geophysics, Colorado School of Mines, Golden, CO 80401-1887

ABSTRACT

Conventional velocity analysis, developed for pure reflection modes recorded on common-midpoint (CMP) gathers, usually cannot be directly applied to converted (PS) waves. The problems are caused by such inherent features of PS-data as the asymmetry of PS-wave moveout in CMP geometry, polarity reversal associated with the zero value of the PS-wave reflection coefficient, and reflection-point dispersal. While the moveout asymmetry generally precludes the use of the conventional hyperbolic moveout equation, the polarity reversal tends to reduce the accuracy of velocity-analysis methods based on the coherency of the reflected signal.

Here, we propose a velocity-analysis technique for converted waves that overcomes some of those problems. The key idea of our method is to resort PS-wave data in such a way that the reflection traveltime becomes symmetric in the vicinity of a chosen source-receiver offset. Since the traveltime usually has a minimum at this offset, we call our procedure "resorting to the traveltime minimum" (RTM) and the corresponding gather – the RTM gather. An important feature of RTM gathers is that they can be built prior to velocity analysis using the slopes of the selected reflection event.

Since the PS-wave moveout of RTM gathers is guaranteed to be locally symmetric, it can be flattened by the conventional hyperbolic moveout equation. Moreover, RTM gathers can be built for an arbitrary offset, allowing one to exclude from velocity analysis source-receiver pairs in the area of the polarity reversal or low signal-to-noise ratio. The value of PS-wave normal-moveout (NMO) velocity obtained from the RTM gathers depends on the velocity structure of the subsurface, and, therefore, can be used to estimate the medium parameters. The correct positions of reflection points for all sources and receivers can be found by migrating PS-data, which solves the problem of reflection point dispersal.

As an example of inversion based on PS-wave NMO velocities, we perform parameter estimation for a homogeneous VTI (transversely isotropic with a vertical symmetry axis) layer above a dipping reflector. We show that traveltimes of P-, PSV-, and PSH-waves reflected from the dipping interface provide unambiguous information about the P- and S-wave vertical velocities, Thomsen anisotropic coefficients ϵ, δ, and γ, and the dip and depth of the reflector.

Key words: converted waves, VTI media, anisotropic parameter estimation

Introduction

Recent technological advances in acquiring multicomponent seismic data made it possible to record converted-wave (PS) reflections on a routine basis. The industry has already recognized that supplementing or replacing conventional P-waves with PS-wave data has a great potential for imaging of hydrocarbon reservoirs, especially beneath gas clouds (Granli et al., 1999; Thomsen,

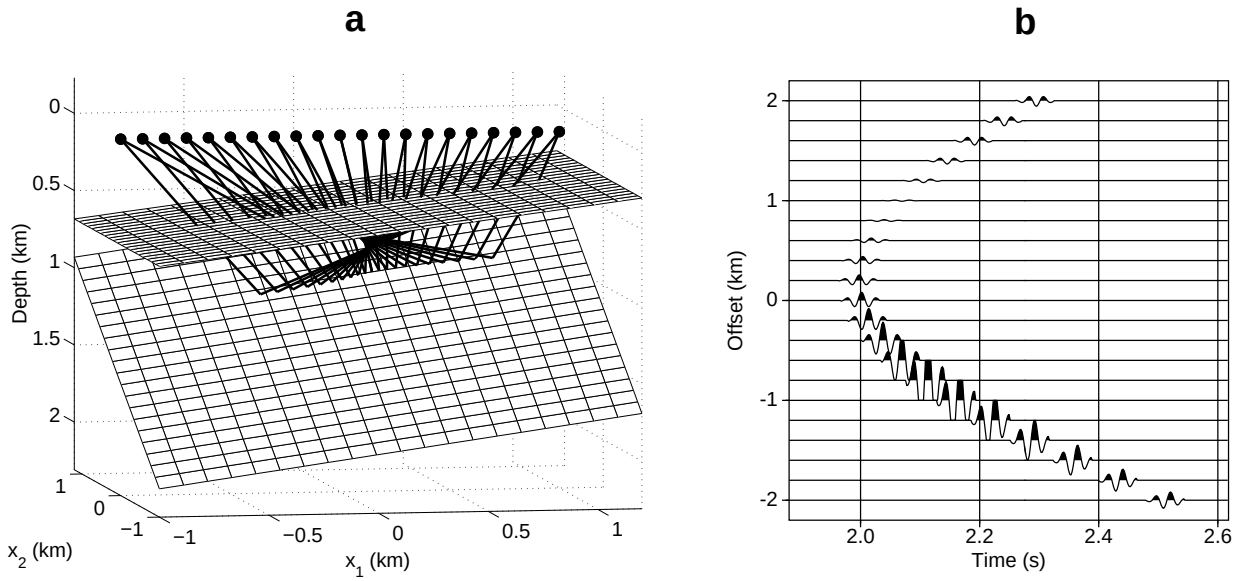

Figure 1. Rays (a) and the horizontal in-line component of a ray-theoretical seismogram (b) of the PSV-wave reflected from the dipping interface below two VTI layers. The relevant layer parameters are: $V_{P0,1} = 1.5$ km/s, $V_{S0,1} = 0.8$ km/s, $\epsilon_1 = 0.15$, $\delta_1 = 0.05$, and $V_{P0,2} = 2.0$ km/s, $V_{S0,2} = 0.9$ km/s, $\epsilon_2 = 0.20$, $\delta_2 = 0.10$. The half-space below the reflector is isotropic with the velocities $V_{P0,3} = 2.2$ km/s and $V_{S0,3} = 1.0$ km/s. The interface dips and azimuths (with respect to the x_1-axis parallel to the CMP line) are: $\phi_1 = 10^\circ$, $\psi_1 = 0^\circ$, and $\phi_2 = 30^\circ$, $\psi_2 = 70^\circ$. The distances of the interfaces from the coordinate origin are: $z_1 = 0.5$ km and $z_2 = 1.2$ km.

1999). The combination of P- and PS-data can be also used to estimate the shear-wave velocities and probably other medium parameters not constrained by P-wave data alone.

Although the advantages of building velocity models based on P- and PS-data seem to be obvious to many geophysicists, there are several specific features of converted modes which hamper direct application to PS-modes of velocity-analysis methods developed for P-waves. The origin of the problem is illustrated by Figure 1 which shows rays and a ray-traced seismogram of a reflected PSV-wave computed for a common-midpoint (CMP) line above a model containing two VTI (transversely isotropic with a vertical symmetry axis) layers. Three features typical for PS-data are obvious in Figure 1:

(1) Positions of the reflection points corresponding to different offsets vary significantly (Figure 1a). One can show that the shift of the reflection point with the offset X (the so-called reflection point dispersal D) is approximately proportional to X. Reflection point dispersal also exists for pure modes; however, in this case $D(X) \sim X^2$ and, for this reason, it can be ignored when offsets are not too large. In contrast, velocity-analysis and imaging methods designed for PS-waves have to deal with reflection point dispersal.

(2) PS-moveout (Figure 1b) is asymmetric with respect to zero offset*. This is the consequence of the well-known fact that the PS-wave reflection traveltime changes if we interchange the source and receiver positions. Clearly, PS-moveout cannot be flattened using conventional semblance analysis based on the hyperbolic moveout equation.

(3) Behavior of the PS-wave amplitude is significantly different at positive and negative offsets. While for $X < 0$ the amplitude varies with offset similarly to what one might expect for pure modes, the striking feature of positive offsets is a change of polarity at $X \approx 1$ km. Such amplitude behavior causes problems for velocity-analysis methods based on any coherency measure of the reflected signal. Although one can account for the polarity change by fitting the amplitude variation together the moveout (Sarkar, Lamb, and Castagna, 1999), this increases the number of unknown parameters and reduces the accuracy of velocity estimation. Another possible solution to this problem might be to exclude from the velocity analysis those offsets where the reflection amplitude is small.

* We conventionally define the offset X as the difference between the receiver r and source s coordinates measured along the CMP line. The offset is positive if $r > s$ and negative otherwise.

Thus, the example in Figure 1 indicates three main inherent problems with PS-data: reflection point dispersal, moveout asymmetry, and the weakness of reflection signal in a certain range of offsets. In this paper, we suggest the following solution of those problems:

First, we select for velocity analysis such portion of PS-moveout where the signal is sufficiently strong and the polarity does not change. (This portion would contain the negative and small positive offsets for the example presented in Figure 1.) This ensures the coherency of the reflection required for reliable application of conventional velocity-analysis methods.

Second, we resort the data to make the moveout symmetric in the vicinity of the chosen (generally nonzero) offset. In contrast to the resorting to the common conversion point (which helps to eliminate reflection point dispersal), our resorting does not require knowledge of any model parameters because it is based solely on the reflection slopes picked from the common-shot and common-receiver sections. Then, we perform conventional velocity analysis on the resorted gathers and find the normal-moveout (NMO) velocity $V_{\mathrm{nmo},PS}$ that flattens the PS-wave moveout.

Third, we invert $V_{\mathrm{nmo},PS}$, along with the P-wave traveltimes, for the relevant model parameters and migrate the PS-wave data. Ideally, this procedure will result in the correct positions of reflection points for each source-receiver pair.

To demonstrate the feasibility of parameter estimation based on dip moveout of converted waves and confirm that the NMO velocity $V_{\mathrm{nmo},PS}$ is sufficiently sensitive to the model parameters, we (similarly to the work of Tsvankin and Grechka, 2000a), estimate the anisotropic coefficients in a homogeneous VTI layer above a dipping reflector using the P-, PSV-, and PSH-reflections. Combining P- and PS-data makes it possible to find all model parameters including reflector depth, whereas P-wave reflection traveltimes alone do not constrain the depth scale in a homogeneous VTI layer (Alkhalifah and Tsvankin, 1995).

Removing the asymmetry of PS moveout

Let us begin by explaining a concept which allows one to apply conventional hyperbolic velocity analysis to PS-wave data. The idea is to resort the data in such a way that reflection traveltime $t(s,r)$ becomes symmetric in the vicinity of any given positions of the source (s^*) and the receiver (r^*). Since the traveltime usually has a minimum at $[s^*,\, r^*]$, we will call this procedure "resorting to the traveltime minimum" (RTM) and the corresponding gather – the RTM gather. In general, such resorting can be performed when the positions $\mathbf{s}^*$ and $\mathbf{r}^*$ are vectors in 3-D space characterized by the Cartesian coordinates $[x_1, x_2, x_3]$ and the source and receiver can move along any direction away from the initial points $\mathbf{s}^*$ and $\mathbf{r}^*$ (see the next section). Here, however, for the purpose of explanation, we restrict ourselves to a 2-D problem and consider $\mathbf{s}$ and $\mathbf{r}$ located on the coordinate axis x_1 (Figure 1a).

We trace the PSV-rays between all sources and receivers (shown in Figure 1a) and obtain the traveltime table $t(s_m, r_n)$, where $m, n = 1, \ldots, N$ and N is the number of the sources and receivers. Figure 2a shows contours of the traveltime t. The gray area indicates the source and receiver positions in the vicinity of the polarity reversal where the reflection amplitude is small. Although we did compute the corresponding traveltimes, they will not be used for velocity analysis. The solid line in Figure 2a shows the coordinates of the sources and receivers which belong to the CMP line with the midpoint at $x_1 = 0$. We know that the PSV-moveout along this line is asymmetric (Figure 1b). At the same time, Figure 2a suggests how to change the source and receive coordinates s and r to symmetrize the moveout. Let us suppose that we want to make the moveout symmetric in the vicinity of zero offset, i.e., near the point $s^* = r^* = 0$. Figure 2a indicates that we should vary s and r along the dashed line which is *tangent* to the traveltime contour at $s^* = r^* = 0$. Figure 2b, which shows the traveltime gradient $\nabla t = \left[\dfrac{\partial t}{\partial r}\,,\ \dfrac{\partial t}{\partial s}\right]$, corroborates our conclusion. Indeed, moving the sources and receivers in the direction *orthogonal* to $\nabla t\Big|_{\substack{s=s^*=0\\ r=r^*=0}}$ ensures that the traveltime $t(s,r)$ has an extremum (usually, a minimum) at $s^* = r^* = 0$. Thus, the dashed lines in Figure 2a and 2b mark the sources and receivers which belong to the RTM gather where the traveltime is symmetric at $s^* = r^* = 0$. To prove that the reflection PS-wave traveltime in RTM geometry is indeed symmetric at $[s^*,\, r^*] = 0$, we computed $t(s,r)$ with s and r varying along the dashed line in Figure 2b. The result presented in Figure 3a clearly demonstrates that $t(s,r)$ has a minimum at the offset $X = 0$.

It is instructive to compare the PS-wave moveout in Figure 3a with that obtained in CMP geometry (Figure 3b). The PS-moveout on the CMP gather is asymmetric (this is also seen directly from the traveltime contours in Figure 2a), with the minimum shifted away from zero offset to $X \approx 0.2$ km. It is obvious that conventional hyperbolic equation cannot flatten such a moveout. Applying this equation to positive and negative offsets separately will result in two different values of the NMO velocity – the phenomenon called by Thomsen (1999) the "diodic velocity". To avoid that, the moveout may be

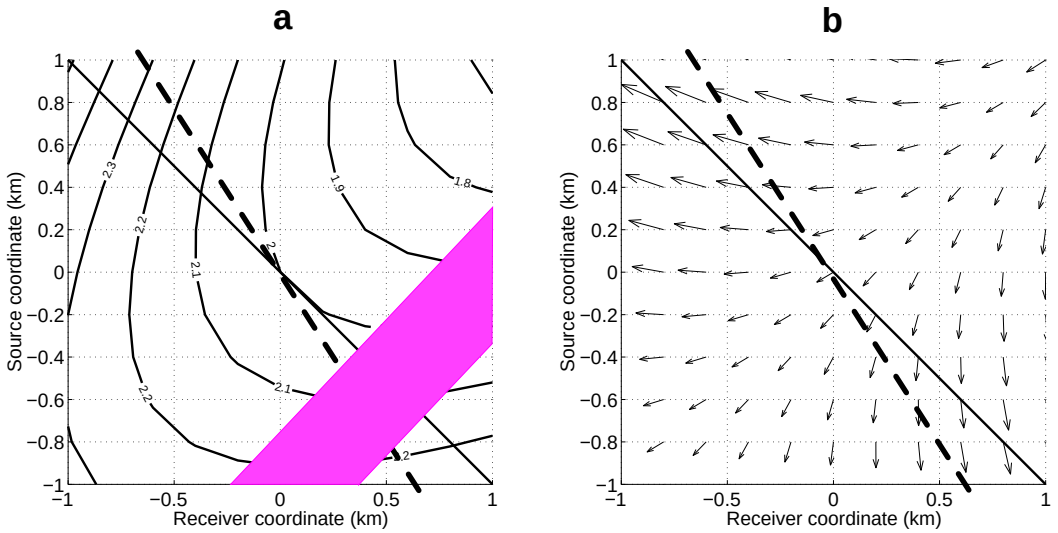

Figure 2. Contours of the reflection PSV-wave traveltime (a) and the traveltime gradient (b) with respect to the source s and receiver r positions for the model in Figure 1a. The gray shade corresponds to the the vicinity of the polarity reversal where the reflection amplitude is small (compare with the seismogram in Figure 1b). The solid lines indicate the sources and receivers on the CMP line in Figure 1a with the midpoint at $x_1 = 0$. The thick dashed lines show the sources and receivers of the resorted gather where the PSV-wave reflection traveltime has a minimum at zero offset.

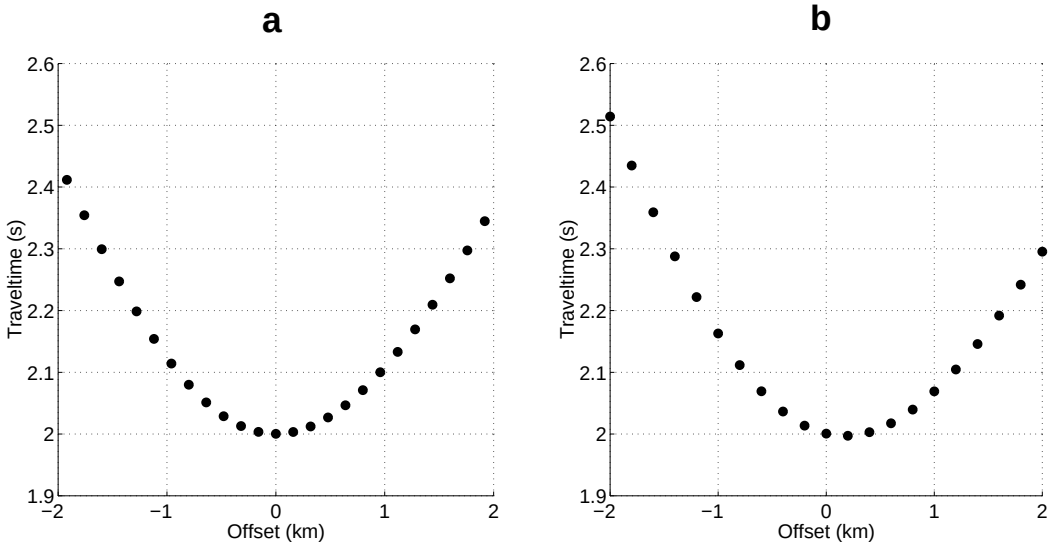

Figure 3. PSV-wave reflection traveltimes in the RTM (a) and CMP (b) geometries computed for the model from Figure 1a.

approximated by a shifted hyperbola, as was discussed by Tsvankin and Grechka (2000a).

In contrast to the CMP gather, the moveout asymmetry is noticeably smaller in the RTM gather (Figure 3a). Below, we show that this "residual" asymmetry, which is mainly related to the presence of the Taylor-series terms of $t(X)$ cubic in the offset X, does not prevent convention velocity analysis from giving correct estimates of the normal-moveout velocity (or the moveout curvature) at $[s^*, r^*]$.

Thus, we have shown that resorting PS-wave data into RTM gathers produces moveouts which are locally symmetric in the vicinity of the chosen source s^* and receiver r^*. Although we have examined only the case when $s^* = r^* = 0$, exactly the same procedure can be applied for nonzero values of s^* and r^*. This is clear from Figure 2a: a straight line tangent to any traveltime contour specifies the RTM gather where the traveltime has a minimum at s^* and r^* corresponding to the tangent point. What we have not discussed yet is *how* to build

the RTM gather or, more specifically, how to obtain the increments s^Δ and r^Δ which are needed to compute the positions of sources $s = s^* + k\,s^\Delta$ $(k = 0, 1, 2, \ldots)$ and receivers $r = r^* + k\,r^\Delta$ on the RTM gather. We will address this issue after presenting a general equation for reflection traveltimes of converted waves.

General equation for converted-wave moveout

Let us examine the behavior of PS-wave reflection traveltime $t(\mathbf{s},\mathbf{r})$ in the vicinity of some point $[\mathbf{s}^*,\mathbf{r}^*]$. The source and receiver coordinates $\mathbf{s}$ and $\mathbf{r}$, as well as $\mathbf{s}^*$ and $\mathbf{r}^*$, are vectors in 3-D space. Assuming the existence of all required derivatives of the function $t(\mathbf{s},\mathbf{r})$, we expand $t(\mathbf{s},\mathbf{r})$ in a Taylor series in the vicinity of $[\mathbf{s}^*,\mathbf{r}^*]$:

$$
\begin{aligned}
t(\mathbf{s},\mathbf{r}) &\equiv t(\mathbf{s}^*+\mathbf{s}^\Delta,\mathbf{r}^*+\mathbf{r}^\Delta)\\
&= t(\mathbf{s}^*,\mathbf{r}^*) + \mathbf{s}^\Delta\cdot\left.\frac{\partial t(\mathbf{s},\mathbf{r}^*)}{\partial\mathbf{s}}\right|_{\mathbf{s}=\mathbf{s}^*}\\
&\quad + \mathbf{r}^\Delta\cdot\left.\frac{\partial t(\mathbf{s}^*,\mathbf{r})}{\partial\mathbf{r}}\right|_{\mathbf{r}=\mathbf{r}^*}\\
&\quad + \frac{1}{2}\,\mathbf{s}^\Delta\left.\frac{\partial^2 t(\mathbf{s},\mathbf{r}^*)}{\partial\mathbf{s}\,\partial\mathbf{s}}\right|_{\mathbf{s}=\mathbf{s}^*}\left(\mathbf{s}^\Delta\right)^{\mathbf{T}}\\
&\quad + \mathbf{s}^\Delta\left.\frac{\partial^2 t(\mathbf{s},\mathbf{r})}{\partial\mathbf{s}\,\partial\mathbf{r}}\right|_{\substack{\mathbf{s}=\mathbf{s}^*\\ \mathbf{r}=\mathbf{r}^*}}\left(\mathbf{r}^\Delta\right)^{\mathbf{T}}\\
&\quad + \frac{1}{2}\,\mathbf{r}^\Delta\left.\frac{\partial^2 t(\mathbf{s}^*,\mathbf{r})}{\partial\mathbf{r}\,\partial\mathbf{r}}\right|_{\mathbf{r}=\mathbf{r}^*}\left(\mathbf{r}^\Delta\right)^{\mathbf{T}}\\
&\quad + O\left[\left(\mathbf{s}^\Delta\right)^m\left(\mathbf{r}^\Delta\right)^{3-m}\right],
\end{aligned}
\tag{1}
$$

where $\mathbf{T}$ denotes transposition.

Although expansion (1) is formal, the meaning of its terms is important for understanding the procedure described below. The quantities $\mathbf{s}^\Delta$ and $\mathbf{r}^\Delta$ are 3-D row-vectors which denote the position of the point $[\mathbf{s},\mathbf{r}] = [\mathbf{s}^*+\mathbf{s}^\Delta,\mathbf{r}^*+\mathbf{r}^\Delta]$ where the traveltime $t(\mathbf{s},\mathbf{r})$ is analyzed. The derivatives $\dfrac{\partial t(\mathbf{s},\mathbf{r}^*)}{\partial\mathbf{s}}$ and $\dfrac{\partial t(\mathbf{s}^*,\mathbf{r})}{\partial\mathbf{r}}$ are 3-D column-vectors with the components $\dfrac{\partial t(\mathbf{s},\mathbf{r}^*)}{\partial s_k}$ and $\dfrac{\partial t(\mathbf{s}^*,\mathbf{r})}{\partial r_k}$ $(k = 1, 2, 3)$, respectively. Since, by definition, the derivatives of traveltime with respect to the spatial coordinates are the components of the slowness vector,

$$
\left.\frac{\partial t(\mathbf{s}^*,\mathbf{r})}{\partial\mathbf{r}}\right|_{\mathbf{r}=\mathbf{r}^*} \equiv \mathbf{p}^{\mathbf{r}} \tag{2}
$$

is the slowness vector measured at the receiver $\mathbf{r}^*$ corresponding to the ray propagating from the source located at $\mathbf{s}^*$. Similarly,

$$
\left.\frac{\partial t(\mathbf{s},\mathbf{r}^*)}{\partial\mathbf{s}}\right|_{\mathbf{s}=\mathbf{s}^*} \equiv \mathbf{p}^{\mathbf{s}} \tag{3}
$$

is the slowness vector of the ray excited at $\mathbf{r}^*$ measured at $\mathbf{s}^*$. For pure reflection modes (which can be treated as a special case of converted modes) examined at zero offset, $\mathbf{r}^* = \mathbf{s}^*$ and, as a consequence, equations (2) and (3) lead to the well-known equality $\mathbf{p}^{\mathbf{r}} = \mathbf{p}^{\mathbf{s}}$. In the case of converted waves, however, $\mathbf{p}^{\mathbf{r}} \neq \mathbf{p}^{\mathbf{s}}$ at any offset.

The terms containing the second-order derivatives in equation (1) are 3×3 matrices with the components,

$$
\left.\frac{\partial^2 t(\mathbf{s},\mathbf{r}^*)}{\partial\mathbf{s}\,\partial\mathbf{s}}\right|_{\mathbf{s}=\mathbf{s}^*} = \left.\frac{\partial^2 t(\mathbf{s},\mathbf{r}^*)}{\partial s_k\,\partial s_m}\right|_{s_k=s_k^*}, \qquad (k,m=1,2,3),\quad \text{etc.} \tag{4}
$$

The physical meaning of those derivatives will be discussed later in the section where we derive an expression for the converted-wave NMO velocity.

The term $O\left[\left(\mathbf{s}^\Delta\right)^m\left(\mathbf{r}^\Delta\right)^{3-m}\right]$ $(m = 0, 1, 2, 3)$ in equation (1) contains the third- and higher-order derivatives of the traveltime t multiplied by the cubic and higher-order products of the components of the vectors $\mathbf{s}^\Delta$ and $\mathbf{r}^\Delta$. Although we will not analyze this term explicitly, we note that for converted modes both even and odd powers of the components s_k^Δ and r_k^Δ are generally present in $O[\ldots]$, whereas in the case of pure modes examined in the vicinity of the zero offset, the odd powers are absent. The asymmetry of the PSV-moveout in Figure 3a, for example, is mainly caused by the presence of the cubic terms in $O[\ldots]$.

PS-wave traveltime in CMP geometry

The moveout equation (1) is the most general local representation of reflection traveltime treated as a scalar function (or scalar field) of six variables: three source coordinates s_k^Δ and three receiver coordinates r_k^Δ. Traveltime in any specific source-receiver geometry can be easily obtained from equation (1) by restricting possible positions of sources and receivers or by relating the vectors $\mathbf{s}^\Delta$ and $\mathbf{r}^\Delta$ to each other. In essence, this is equivalent to making a certain cross-section of the six-dimensional traveltime field $t(\mathbf{s}^\Delta,\mathbf{r}^\Delta)$.

Here, we derive an equation describing PS-wave reflection moveout in the vicinity of the common midpoint

$$
\mathbf{s}^* = \mathbf{r}^* \equiv \mathbf{y}^* \tag{5}
$$

along the CMP line oriented parallel to the unit vector $\boldsymbol{\ell}$. Let us denote the offset X_ℓ^Δ and suppose that the receiver moves in the direction of $\boldsymbol{\ell}$ while the source moves in the opposite direction. Then, the receiver and source displacements along $\boldsymbol{\ell}$ are

$$
\mathbf{r}^\Delta = \frac{X_\ell^\Delta}{2}\,\boldsymbol{\ell} \tag{6}
$$

and

$$
\mathbf{s}^\Delta = -\frac{X_\ell^\Delta}{2}\,\boldsymbol{\ell}. \tag{7}
$$

Substituting equations (5)–(7) along with the definitions of the slowness vectors (2) and (3) into formula (1) yields

$$t(\mathbf{y}^*,\ell,X_\ell^\Delta)=t(\mathbf{y}^*)+\ell\cdot(\mathbf{p}^{\mathbf{r}}-\mathbf{p}^{\mathbf{s}})\ \frac{X_\ell^\Delta}{2} + \ell\left(\left.\frac{\partial^2 t(\mathbf{s},\mathbf{y}^*)}{\partial\mathbf{s}\,\partial\mathbf{s}}\right|_{\mathbf{s}=\mathbf{y}^*} - 2\left.\frac{\partial^2 t(\mathbf{s},\mathbf{r})}{\partial\mathbf{s}\,\partial\mathbf{r}}\right|_{\substack{\mathbf{s}=\mathbf{y}^*\\ \mathbf{r}=\mathbf{y}^*}} + \left.\frac{\partial^2 t(\mathbf{y}^*,\mathbf{r})}{\partial\mathbf{r}\,\partial\mathbf{r}}\right|_{\mathbf{r}=\mathbf{y}^*}\right)\ell^{\mathbf{T}}\,\frac{(X_\ell^\Delta)^2}{8} + O\left[(X_\ell^\Delta)^3\right]. \tag{8}$$

The presence of the term $\ell\cdot(\mathbf{p}^{\mathbf{r}}-\mathbf{p}^{\mathbf{s}})\ X_\ell^\Delta/2$ linear in X_ℓ^Δ is the main reason for the asymmetry of PS-moveout in CMP geometry (see Figure 3b).

Clearly, squaring equation (8) cannot eliminate the linear term and, consequently, this moveout cannot be described by the conventional hyperbolic moveout equation. Still, such moveout attributes as the traveltime slope at zero offset, the shift of the traveltime minimum, and the moveout curvature can be used for parameter estimation as was done by Tsvankin and Grechka (2000a, 2000b) for layered VTI media. The same procedure can be extended to more complicated subsurface models.

Note that the linear term in equation (8) vanishes for pure reflection modes due to the equality $\mathbf{p}^{\mathbf{r}}=\mathbf{p}^{\mathbf{s}}$. In this case, the quadratic term is related to the pure-mode NMO velocity along the CMP line ℓ and can be shown to be equivalent to that obtained by Grechka and Tsvankin (1998).

Building RTM gathers

Using equation (1), the source and receiver displacements ($\mathbf{s}^\Delta$ and $\mathbf{r}^\Delta$) can be related in such a way that the traveltime t has an extremum at $[\mathbf{s}^*,\mathbf{r}^*]$. By definition, t reaches its extremum at $[\mathbf{s}^*,\mathbf{r}^*]$ if the Taylor series expansion (1) does not contain linear terms. Taking into account equations (2) and (3), we obtain the following condition

$$\mathbf{s}^\Delta\cdot\mathbf{p}^{\mathbf{s}}+\mathbf{r}^\Delta\cdot\mathbf{p}^{\mathbf{r}}=0. \tag{9}$$

Equation (9) may be interpreted as the constraint on the mutual displacements of the sources and receivers that ensures the existence of a traveltime extremum at $[\mathbf{s}^*,\mathbf{r}^*]$.

Suppose, we specify the source displacement $\mathbf{s}^\Delta$ and would like to obtain the corresponding $\mathbf{r}^\Delta$. Clearly, equation (9) provides only one relation for three components r_k^Δ and, as a consequence, those components cannot be found uniquely. As a simple example, consider a pure-mode zero-offset ray reflected from a horizontal interface below a laterally homogeneous medium. In this case, as we know, $\mathbf{p}^{\mathbf{r}}=\mathbf{p}^{\mathbf{s}}=[0,0,p_3]$. Thus, arbitrary receiver and source displacements $\mathbf{r}^\Delta$ and $\mathbf{s}^\Delta$ in the horizontal plane, as well as those satisfying the constraint $r_3^\Delta+s_3^\Delta=0$, will satisfy equation (9).

The inherent nonuniqueness of condition (9) can be eliminated if we allow the receiver and source to move only in certain directions, say $\ell^{\mathbf{r}}$ and $\ell^{\mathbf{s}}$ (i.e., $\mathbf{r}^\Delta=r_{\ell^{\mathbf{r}}}^\Delta\,\ell^{\mathbf{r}}$ and $\mathbf{s}^\Delta=s_{\ell^{\mathbf{s}}}^\Delta\,\ell^{\mathbf{s}}$). Then equation (9) becomes

$$s_{\ell^{\mathbf{s}}}^\Delta\,\ell^{\mathbf{s}}\cdot\mathbf{p}^{\mathbf{s}}+r_{\ell^{\mathbf{r}}}^\Delta\,\ell^{\mathbf{r}}\cdot\mathbf{p}^{\mathbf{r}}=0. \tag{10}$$

Equation (10) relates two scalar quantities $s_{\ell^{\mathbf{s}}}^\Delta$ and $r_{\ell^{\mathbf{r}}}^\Delta$ and, therefore, can be solved uniquely if one of those quantities is specified.

The most practically important case, which we are going to examine in detail, is when

$$\ell^{\mathbf{s}}=\ell^{\mathbf{r}}\equiv\ell, \tag{11}$$

i.e., when the sources and receivers move along the same line ℓ. Denoting the source and receiver displacements along ℓ by s_ℓ^Δ and r_ℓ^Δ, we rewrite equation (10) in the form:

$$r_\ell^\Delta\,\ell\cdot\mathbf{p}^{\mathbf{r}}=-s_\ell^\Delta\,\ell\cdot\mathbf{p}^{\mathbf{s}}. \tag{12}$$

The minus sign in equation (12) indicates that one of the directional traveltime derivatives, which define the slownesses $\mathbf{p}^{\mathbf{r}}$ and $\mathbf{p}^{\mathbf{s}}$ [see equations (2) and (3)], has to be taken in the direction *opposite* to the actual displacement of the receiver or the source. Therefore, we need either to redefine one of slownesses ($\mathbf{p}^{\mathbf{r}}$ or $\mathbf{p}^{\mathbf{s}}$) or to incorporate the minus sign into one of the projections ($\ell\cdot\mathbf{p}^{\mathbf{r}}$ or $\ell\cdot\mathbf{p}^{\mathbf{s}}$) of the slowness vectors onto line ℓ. The latter option is more attractive because it allows us to keep equations developed so far unchanged. Selecting this option we have to remember, however, that the receiver and source move in the opposite directions when the ratio $\dfrac{\ell\cdot\mathbf{p}^{\mathbf{r}}}{\ell\cdot\mathbf{p}^{\mathbf{s}}}>0$ and in the same direction when $\dfrac{\ell\cdot\mathbf{p}^{\mathbf{r}}}{\ell\cdot\mathbf{p}^{\mathbf{s}}}<0$. For example, if the receiver displacement is directed along ℓ, the slowness projections can be defined as

$$p_\ell^{\mathbf{r}}=\ell\cdot\mathbf{p}^{\mathbf{r}} \tag{13}$$

and

$$p_\ell^{\mathbf{s}}=-\ell\cdot\mathbf{p}^{\mathbf{s}}. \tag{14}$$

If the source moves along ℓ, then we define

$$p_\ell^{\mathbf{r}}=-\ell\cdot\mathbf{p}^{\mathbf{r}} \tag{15}$$

and

$$p_\ell^{\mathbf{s}}=\ell\cdot\mathbf{p}^{\mathbf{s}}. \tag{16}$$

Either of the definitions (13) and (14), or (15) and (16) lead to the following form of equation (12):

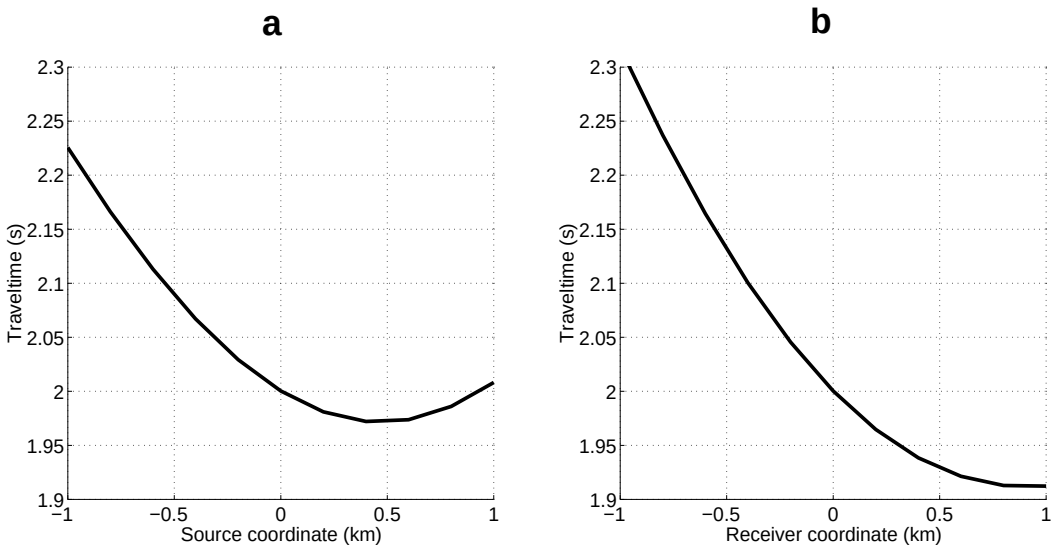

Figure 4. Traveltimes of the PSV-reflection from Figure 1a resorted (a) into the common-receiver gather at $r^* = 0$ and (b) into the common-shot gather at $s^* = 0$.

$$\frac{s_\ell^\Delta}{r_\ell^\Delta} = \frac{p_\ell^{\mathbf{r}}}{p_\ell^{\mathbf{s}}}. \tag{17}$$

Equation (17) allows us to construct the RTM gather along the line ℓ. For instance, for pure modes at zero offset $p_\ell^{\mathbf{r}} = p_\ell^{\mathbf{s}}$. In this case, equation (17) yields $s_\ell^\Delta = r_\ell^\Delta$. This condition defines a CMP gather: the source and receiver move in the opposite directions and their displacements with respect to the common midpoint are equal. Thus, CMP gathers can be viewed as a special case of RTM gathers for pure-mode reflections. Equation (17) however, is more general and can be used to build symmetric moveout functions for either pure or converted modes at any offset. The importance of this equation for practical applications is due to the fact that the slownesses $p_\ell^{\mathbf{s}}$ and $p_\ell^{\mathbf{r}}$ are simply the *slopes* of the examined reflection event on the *common-receiver* and *common-shot* sections measured at points $\mathbf{s}^*$ and $\mathbf{r}^*$. Therefore, the quantities $p_\ell^{\mathbf{s}}$ and $p_\ell^{\mathbf{r}}$ can be picked directly from reflection data.

Equation (17) also shows a serious drawback of the approach based on RTM gathers. Since the ratio $\frac{s_\ell^\Delta}{r_\ell^\Delta}$ is equal to the ratio of the reflection slopes $p_\ell^{\mathbf{r}}$ and $p_\ell^{\mathbf{s}}$ at $[\mathbf{s}^*, \mathbf{r}^*]$, the source and receiver increments s_ℓ^Δ and r_ℓ^Δ generally depend on the coordinates $\mathbf{s}^*$ and $\mathbf{r}^*$. This implies that the procedure of building RTM gathers (that essentially amounts to resorting the data) has to be performed at each pair $[\mathbf{s}^*, \mathbf{r}^*]$ along line ℓ. It is also clear that one has to construct different RTM gathers for reflection events from different interfaces, even if the gathers are located at the same point $[\mathbf{s}^*, \mathbf{r}^*]$.

To show an example of the RTM building procedure, we resorted the traveltimes of the PSV-reflection computed for the model in Figure 1a into common-receiver and common-shot gathers (Figure 4). The gathers were obtained for the common receiver at $r^* = 0$ and the common source at $s^* = 0$ (compare Figure 4 with the cross-sections of the contours in Figure 2a by the lines $r = r^* = 0$ and $s = s^* = 0$). The traveltime slopes measured at $s^* = 0$ and $r^* = 0$ are the slownesses $p_1^{\mathbf{s}}$ and $p_1^{\mathbf{r}}$ (the subscript "1" denotes that the line is directed along the x_1-axis). Measuring those slopes in Figure 4a and 4b, we find $p_1^{\mathbf{s}} = -0.12$ s/km and $p_1^{\mathbf{r}} = -0.20$ s/km. From equation (17) we compute the ratio of the source and receiver increments $s_1^\Delta / r_1^\Delta = 1.67$, which was used to construct the RTM gather and obtain the traveltimes shown in Figure 3a.

Thus, the information needed for building RTM gathers is contained in the reflection traveltimes of converted waves, specifically, in the common-shot and common-receiver sections. Next, we continue analysis of equation (1) and derive the normal-moveout velocity of PS-waves in RTM geometry.

NMO velocity on RTM gathers

Suppose we recorded a reflected PS-wave along the line ℓ and resorted the data into an RTM gather so that the PS-moveout became symmetric at the chosen point $[\mathbf{s}^*, \mathbf{r}^*]$. Then, we can perform conventional velocity analysis to obtain the normal-moveout velocity at $[\mathbf{s}^*, \mathbf{r}^*]$. Here, we derive an analytic expression for the PS-wave NMO velocity $V_{\mathrm{nmo},PS}$ using the Taylor series (1).

According to our sign convention [see equations (12)–(17) and the related discussion], the offset in-

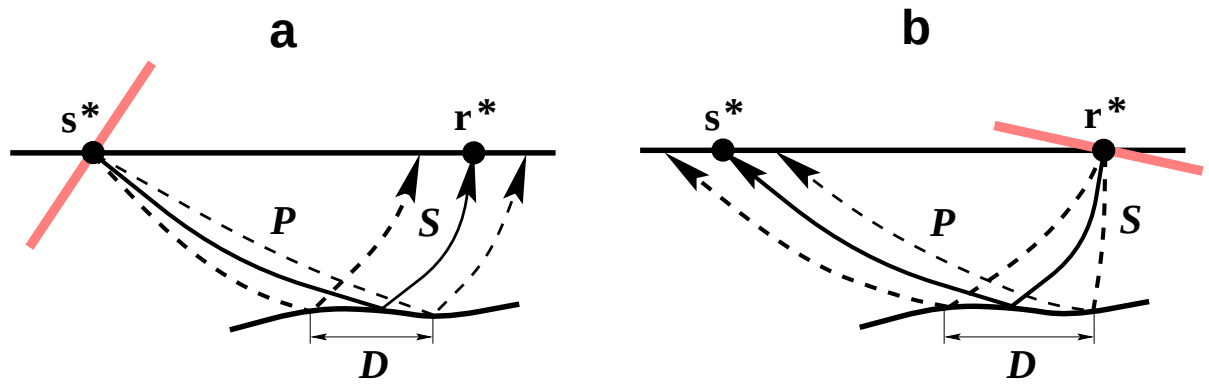

Figure 5. Reflected PS-rays in common-shot (a) and common-receiver (b) geometries can be treated as one-way rays corresponding to the nonexistent reflectors (gray lines) located at common shot $\mathbf{s}^*$ and common receiver $\mathbf{r}^*$. D denotes reflection point dispersal.

crement X_ℓ^Δ should be defined as the sum of the receiver and source increments r_ℓ^Δ and s_ℓ^Δ:

$$X_\ell^\Delta = r_\ell^\Delta + s_\ell^\Delta . \tag{18}$$

Using equation (17), X_ℓ^Δ can be rewritten in terms of either s_ℓ^Δ or r_ℓ^Δ as

$$X_\ell^\Delta = r_\ell^\Delta \left(1 + \frac{p_\ell^{\mathbf{r}}}{p_\ell^{\mathbf{s}}}\right) = s_\ell^\Delta \left(1 + \frac{p_\ell^{\mathbf{s}}}{p_\ell^{\mathbf{r}}}\right) . \tag{19}$$

Solving equations (19) for the source and receiver increments yields

$$\mathbf{s}^\Delta = s_\ell^\Delta \ell = \frac{p_\ell^{\mathbf{r}} X_\ell^\Delta}{p_\ell^{\mathbf{s}} + p_\ell^{\mathbf{r}}}\, \ell \tag{20}$$

and

$$\mathbf{r}^\Delta = r_\ell^\Delta \ell = \frac{p_\ell^{\mathbf{s}} X_\ell^\Delta}{p_\ell^{\mathbf{s}} + p_\ell^{\mathbf{r}}}\, \ell . \tag{21}$$

Next we substitute equations (20) and (21) into the Taylor series expansion (1) and represent it in the form:

$$\begin{aligned} t(\mathbf{s},\mathbf{r}) \equiv t(\mathbf{s}^*,\mathbf{r}^*,\ell,X_\ell^\Delta) = t^* \\ + \frac{1}{2}\,\ell\, \frac{\partial^2 t(\mathbf{s},\mathbf{r}^*)}{\partial \mathbf{s}\,\partial \mathbf{s}}\bigg|_{\mathbf{s}=\mathbf{s}^*} \ell^{\mathbf{T}} \left(\frac{p_\ell^{\mathbf{r}} X_\ell^\Delta}{p_\ell^{\mathbf{s}} + p_\ell^{\mathbf{r}}}\right)^2 \\ + \ell\, \frac{\partial^2 t(\mathbf{s},\mathbf{r})}{\partial \mathbf{s}\,\partial \mathbf{r}}\bigg|_{\substack{\mathbf{s}=\mathbf{s}^* \\ \mathbf{r}=\mathbf{r}^*}} \ell^{\mathbf{T}} p_\ell^{\mathbf{r}}\, p_\ell^{\mathbf{s}} \left(\frac{X_\ell^\Delta}{p_\ell^{\mathbf{s}} + p_\ell^{\mathbf{r}}}\right)^2 \\ + \frac{1}{2}\,\ell\, \frac{\partial^2 t(\mathbf{s}^*,\mathbf{r})}{\partial \mathbf{r}\,\partial \mathbf{r}}\bigg|_{\mathbf{r}=\mathbf{r}^*} \ell^{\mathbf{T}} \left(\frac{p_\ell^{\mathbf{s}} X_\ell^\Delta}{p_\ell^{\mathbf{s}} + p_\ell^{\mathbf{r}}}\right)^2 \\ + O\left[\left(X_\ell^\Delta\right)^3\right] , \end{aligned} \tag{22}$$

where $t^* \equiv t(\mathbf{s}^*,\mathbf{r}^*)$. Squaring equation (22) yields

$$\begin{aligned} t^2(\mathbf{s}^*,\mathbf{r}^*,\ell,X_\ell^\Delta) = (t^*)^2 + \left(\frac{X_\ell^\Delta}{V_{\mathrm{nmo},PS}(\mathbf{s}^*,\mathbf{r}^*,\ell)}\right)^2 \\ + O\left[\left(X_\ell^\Delta\right)^3\right] , \end{aligned} \tag{23}$$

where the converted-wave NMO velocity is

$$\begin{aligned} V_{\mathrm{nmo},PS}^{-2}(\mathbf{s}^*,\mathbf{r}^*,\ell) = \\ \frac{t^*}{(p_\ell^{\mathbf{s}} + p_\ell^{\mathbf{r}})^2}\, \ell \left\{ \frac{\partial^2 t(\mathbf{s},\mathbf{r}^*)}{\partial \mathbf{s}\,\partial \mathbf{s}}\bigg|_{\mathbf{s}=\mathbf{s}^*} (p_\ell^{\mathbf{r}})^2 \right. \\ + 2\, \frac{\partial^2 t(\mathbf{s},\mathbf{r})}{\partial \mathbf{s}\,\partial \mathbf{r}}\bigg|_{\substack{\mathbf{s}=\mathbf{s}^* \\ \mathbf{r}=\mathbf{r}^*}} p_\ell^{\mathbf{r}}\, p_\ell^{\mathbf{s}} \\ \left. + \frac{\partial^2 t(\mathbf{s}^*,\mathbf{r})}{\partial \mathbf{r}\,\partial \mathbf{r}}\bigg|_{\mathbf{r}=\mathbf{r}^*} (p_\ell^{\mathbf{s}})^2 \right\} \ell^{\mathbf{T}} . \end{aligned} \tag{24}$$

To simplify this expression, we need to discuss the physical meaning of the second-order traveltime derivatives $\partial^2 t/(\partial \mathbf{s}\,\partial \mathbf{s})$, $\partial^2 t/(\partial \mathbf{s}\,\partial \mathbf{r})$, and $\partial^2 t/(\partial \mathbf{r}\,\partial \mathbf{r})$.

The derivative

$$\frac{\partial^2 t(\mathbf{s}^*,\mathbf{r})}{\partial \mathbf{r}\,\partial \mathbf{r}}\bigg|_{\mathbf{r}=\mathbf{r}^*} = \frac{\partial^2 t(\mathbf{s}^*,\mathbf{r})}{\partial r_k\,\partial r_m}\bigg|_{r_k=r_k^*} , \qquad (k,m=1,2,3) \tag{25}$$

is calculated for rays shot from the source at $\mathbf{s}^*$ to different receivers in the vicinity of $\mathbf{r}^*$. Note that the traveltime $t(\mathbf{s}^*,\mathbf{r})$ can be interpreted as the *one-way* reflection traveltime of the ray reflected from a *nonexistent* reflector at $\mathbf{s}^*$ (Figure 5a). The traveltimes recorded for the receivers at $\mathbf{r}^* - \mathbf{r}^\Delta$ and $\mathbf{r}^* + \mathbf{r}^\Delta$ can be summed up to produce a synthetic CMP gather with the midpoint at $\mathbf{r}^*$. Since the "reflection point" $\mathbf{s}^*$ stays the same for all the rays within this synthetic gather, the derivative $\dfrac{\partial^2 t}{\partial \mathbf{r}\,\partial \mathbf{r}}$ can be found from the theory of the NMO-velocity surfaces $\mathbf{U}$ developed by Grechka and Tsvankin (1999):

$$\frac{\partial^2 t(\mathbf{s}^*,\mathbf{r})}{\partial \mathbf{r}\,\partial \mathbf{r}}\bigg|_{\mathbf{r}=\mathbf{r}^*} = \frac{\mathbf{U}^{\mathbf{r}}}{t^*} , \tag{26}$$

where the superscript "$\mathbf{r}$" in $\mathbf{U}^{\mathbf{r}}$ denotes that the NMO-velocity surface corresponds to the receiver. The reflec-

tion point dispersal D (Figure 5a) is automatically incorporated into computation of the NMO-velocity surface $\mathbf{U^r}$.

Similar relations can be written for the derivative $\dfrac{\partial^2 t}{\partial \mathbf{s}\,\partial \mathbf{s}}$ [equation (24)] which relates to the NMO-velocity surface $\mathbf{U^s}$ that would be measured in a synthetic CMP gather constructed for rays that have the common receiver $\mathbf{r}^*$ (Figure 5b). By analogy with equation (26), we obtain

$$\left.\frac{\partial^2 t(\mathbf{s},\mathbf{r}^*)}{\partial \mathbf{s}\,\partial \mathbf{s}}\right|_{\mathbf{s}=\mathbf{s}^*} = \frac{\mathbf{U^s}}{t^*}\,. \tag{27}$$

Thus, substituting equations (26) and (27) into (24) yields

$$V^{-2}_{\mathrm{nmo},PS}(\mathbf{s}^*,\mathbf{r}^*,\ell) = \frac{1}{(p^{\mathbf{s}}_\ell + p^{\mathbf{r}}_\ell)^2} \tag{28}$$

$$\times \ell \left\{ \mathbf{U^s}\,(p^{\mathbf{r}}_\ell)^2 + 2\,\left.\frac{\partial^2 t(\mathbf{s},\mathbf{r})}{\partial \mathbf{s}\,\partial \mathbf{r}}\right|_{\substack{\mathbf{s}=\mathbf{s}^*\\ \mathbf{r}=\mathbf{r}^*}} t^*\,p^{\mathbf{r}}_\ell\,p^{\mathbf{s}}_\ell + \mathbf{U^r}\,(p^{\mathbf{s}}_\ell)^2 \right\} \ell^{\mathbf{T}}.$$

This is the final expression for the NMO velocity measured on the RTM gather. Note that the reflection point dispersal D, which is approximately proportional to the offset increment X^{Δ}_{ℓ} for either common-shot or common-receiver gathers (Figure 5), is automatically taken into account in computing the NMO-velocity surfaces $\mathbf{U^r}$, $\mathbf{U^s}$ and the traveltime derivative $\dfrac{\partial^2 t}{\partial \mathbf{s}\,\partial \mathbf{r}}$. For example, all those quantities depend on the reflector curvature and on its dip and azimuth at the reflection point. Thus, the influence of the reflection point dispersal on the PS-wave traveltime on RTM gathers is hidden in the NMO velocity $V_{\mathrm{nmo},PS}$.

Equation (28) is valid for arbitrary heterogeneous anisotropic media. It cannot be simplified any further without making some assumptions about the model. The reason is that, in general, the mixed traveltime derivative $\dfrac{\partial^2 t}{\partial \mathbf{s}\,\partial \mathbf{r}}$ cannot be expressed in terms of the NMO-velocity surfaces $\mathbf{U}$. We suggest evaluating this derivative numerically (through finite differences) based on the definition of the slowness vector $\mathbf{p^s}$ [equation (3)]

$$\left.\frac{\partial^2 t(\mathbf{s},\mathbf{r})}{\partial \mathbf{s}\,\partial \mathbf{r}}\right|_{\substack{\mathbf{s}=\mathbf{s}^*\\ \mathbf{r}=\mathbf{r}^*}} = \left.\frac{\partial \mathbf{p^s}}{\partial \mathbf{r}}\right|_{\mathbf{r}=\mathbf{r}^*}. \tag{29}$$

Azimuthal variation of $V_{\mathrm{nmo},PS}$ at zero offset ($\mathbf{s}^* = \mathbf{r}^*$)

Equation (28) allows us to make an important observation about the dependence of the NMO velocity $V_{\mathrm{nmo},PS}$ of the direction of the line ℓ. If the vector ℓ is confined to the horizontal plane, i.e.,

$$\ell = [\cos\alpha,\ \sin\alpha,\ 0]\,, \tag{30}$$

where α is the azimuth, the function $V_{\mathrm{nmo},PS}(\alpha)$ describes the azimuthal variation of the PS-wave NMO velocity. In contrast to the azimuthal dependence of the pure-mode NMO velocity, which is known to be elliptical (Grechka and Tsvankin, 1998), the function $V_{\mathrm{nmo},PS}(\alpha)$ is generally *not* an ellipse. This conclusion follows directly from equation (28) because, although the matrices $\mathbf{U^r}$ and $\mathbf{U^s}$ are symmetric (Grechka and Tsvankin, 1999), the matrix $\dfrac{\partial^2 t}{\partial \mathbf{s}\,\partial \mathbf{r}}$ is generally not. Also, additional azimuthal dependence is hidden in the slowness components $p^{\mathbf{r}}_\ell$ and $p^{\mathbf{s}}_\ell$. Thus, the NMO velocity $V_{\mathrm{nmo},PS}(\alpha)$ has an oval shape which may or may not be close to an ellipse.

An important special case is that of horizontally layered anisotropic media where all layers have a horizontal symmetry plane. In this case, PS-wave reflection traveltime is symmetric in CMP geometry and, therefore, any CMP gather coincides with the RTM gather at $\mathbf{s}^* = \mathbf{r}^*$. The azimuthal variation of the NMO velocity in CMP geometry in this model was studied by Grechka, Theophanis, and Tsvankin (1999), who showed that $V_{\mathrm{nmo},PS}(\alpha)$ is always an ellipse.

Homogeneous layer above plane dipping reflector

The function $V_{\mathrm{nmo},PS}(\alpha)$ also describes an ellipse in the model that contains a single homogeneous anisotropic layer above a plane dipping reflector. In this case, as shown in Appendix A,

$$U^{\mathbf{r}}_{ij} = U^{\mathbf{s}}_{ij} = t^*\,\left.\frac{\partial^2 t(\mathbf{s},\mathbf{r})}{\partial s_i\,\partial r_j}\right|_{\substack{\mathbf{s}=\mathbf{s}^*=\\ \mathbf{r}=\mathbf{r}^*}}, \qquad (i,j=1,2)\,, \tag{31}$$

and equation (28) reduces to

$$V^{-2}_{\mathrm{nmo},PS}(\mathbf{s}^*=\mathbf{r}^*,\alpha) = \ell\,\mathbf{U^r}\ell^{\mathbf{T}} = \ell\,\mathbf{U^s}\ell^{\mathbf{T}}\,, \tag{32}$$

where ℓ is given by (30). Equation (32) is identical to the expression for the pure-mode NMO velocity (Grechka and Tsvankin, 1999), which proves that the azimuthal variation of $V_{\mathrm{nmo},PS}$ is elliptical.

Numerical example

Let us use the model from Figure 1a to verify the accuracy of equation (28) that describes the PS-wave NMO velocity. Since the reflection amplitude for some offsets is small, it might be reasonable to exclude such source-receiver pairs (indicated by the gray shading in Figure 2a) from velocity analysis. Thus, we have selected the RTM gather shown with the dashed line in Figure 6. Note that the initial source and receiver positions $s^*_1 = 0$ and $r^*_1 = -0.7$ km correspond to the *nonzero* offset $X^*_1 = -0.7$ km. Also, according to the positive slope of the dashed line in Figure 6, the sources and receivers within this RTM gather move in the *same* direction.

The PSV-wave reflection traveltime t as a function of the offset increment X^{Δ}_1 (the offset is equal to the

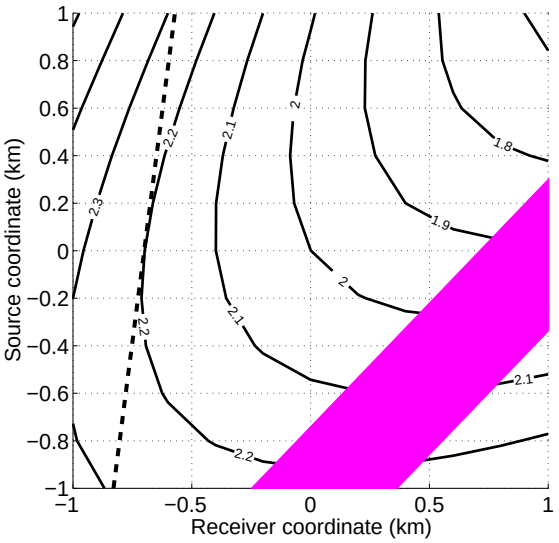

Figure 6. Contours of the PSV-wave reflection traveltime from Figure 2a and the RTM gather (dashed) selected for velocity analysis.

difference $X_1^{\Delta} - X_1^*$) is displayed in Figure 7a. Clearly, the traveltime $t\left(X_1^{\Delta}\right)$ has a minimum at $X_1^{\Delta} = 0$. At greater offset increments, however, it becomes evident that the moveout is asymmetric, which is not surprising because equation (22) for $t\left(X_1^{\Delta}\right)$ contains odd powers of X_1^{Δ}.

To perform conventional hyperbolic velocity analysis, one would fit the squared traveltime $t^2\left(\left[X_1^{\Delta}\right]^2\right)$ to a straight line (Figure 7b). The presence of the odd (mostly cubic) terms in the traveltime series [equation (23)] leads to a "swallow-tail" shape of the function $t^2\left(\left[X_1^{\Delta}\right]^2\right)$. In general, such a shape of the traveltime function may cause problems for velocity analysis, especially if it is done separately for the moveout branches corresponding to positive and negative offset increments. However, the influence of odd powers of X_1^{Δ} on the NMO-velocity estimate can be eliminated if the offset increments are such that $\max\left(X_1^{\Delta}\right) = -\min\left(X_1^{\Delta}\right)$. In this case, the odd terms in X_1^{Δ} cancel each other and, similarly to pure modes, only the nonhyperbolic moveout has to be accounted for. Its influence, though, is known to be insignificant (i.e., Tsvankin and Thomsen, 1994), as long as the spreadlength-to-depth ratio does not exceed unity. Since this is the case in our example, the hyperbolic moveout approximation should be sufficiently accurate (Figure 7b). The difference between the theoretical NMO velocity computed using equation (28) [the theoretical hyperbolic moveout is marked by the crosses] and the best-fit NMO velocity calculated from the slope of the straight line in Figure 7b is 0.4%. Thus, conventional moveout analysis can be used for converted waves resorted into RTM gathers.

Parameter estimation in VTI media

The PS-wave NMO velocities obtained from RTM gathers, as well as such moveout attributes as the slowness components $p_\ell^{\mathbf{s}}$, $p_\ell^{\mathbf{r}}$, and traveltime t^* provide valuable information for parameter estimation. Here, we analyze the joint inversion of P-, PSV-, and PSH-reflections from a dipping interface below a homogeneous VTI layer. Tsvankin and Grechka (2000a), who examined a similar problem in 2-D, concluded that the presence of P- and PSV-reflections from horizontal *and* dipping interfaces is required for stable estimation of the vertical velocities V_{P0} and V_{S0}, and Thomsen's (1986) anisotropic coefficients ϵ and δ. Since the formalism developed in this paper allows us to compute PS-wave NMO velocities along arbitrarily oriented lines ℓ, we will perform the inversion in 3-D. Similarly to the results of Tsvankin and Grechka (2000b), we will show that the azimuthal dependence of P- and PS-wave NMO velocities from a single dipping reflector provides unambiguous information about the model parameters.

Combination of P and PSV data

We start by inverting the traveltimes of P- and PSV-waves. The azimuthal variation of the P-wave NMO velocity (the NMO ellipse) from a dipping reflector can be used to estimate two quantities: the zero-dip P-wave NMO velocity $V_{\mathrm{nmo},P}(0) = V_{P0}\sqrt{1+2\,\delta}$ and the anellipticity coefficient $\eta \equiv \dfrac{\epsilon-\delta}{1+2\,\delta}$ (Grechka and Tsvankin, 1998). Therefore, at least two more constraints are needed to obtain all four relevant parameters (V_{P0}, V_{S0}, ϵ, and δ) responsible for P- and PSV-wave kinematics in VTI media. Tsvankin and Grechka (2000a) showed that the addition of PSV-moveout from a horizontal reflector to $V_{\mathrm{nmo},P}(0)$ and η determined from P-wave data does not produce a stable inversion scheme. Therefore, it is necessary to include a PSV-reflection from a dipping interface. In essence, such a reflection is required to produce rays which propagate within a different range of spatial directions and, as a consequence, provide an additional constraint on the model parameters. Here, the same goal will be achieved by using the PSV-wave NMO velocities on RTM gathers corresponding to different initial offsets X^*.

Our data for the inversion test presented in Figure 8 included:

(i) P-wave NMO ellipse.

(ii) PSV-wave NMO ellipse at zero offset $X^* = 0$ [equation (32)].

(iii) The dip-direction PSV-wave NMO velocities at four initial offsets $X^* = [-z/2,\ -z/4,\ z/4,\ z/2]$ [equa-

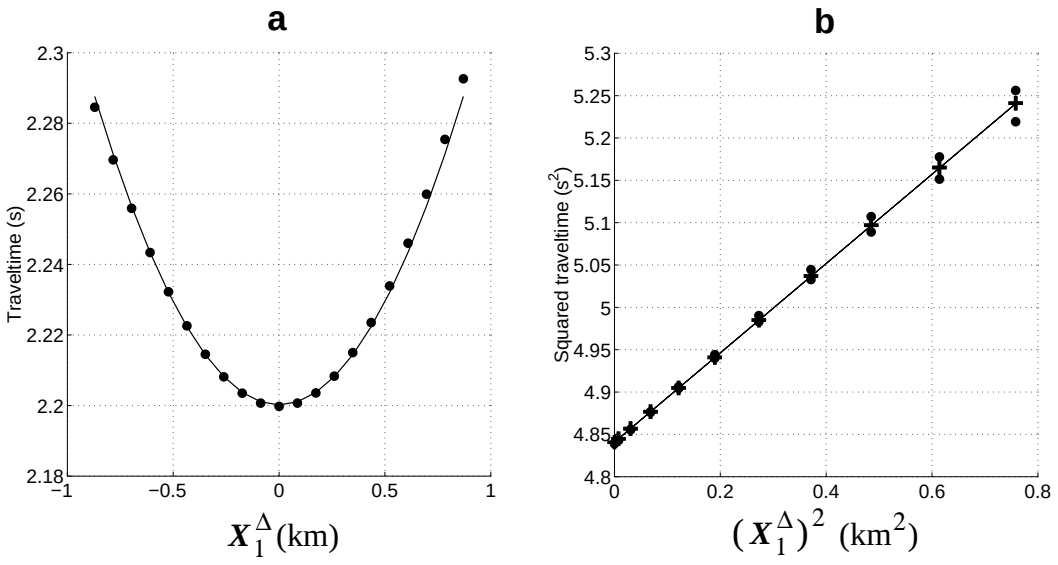

Figure 7. (a) Dots – PSV-wave reflection traveltime $t(X_1^\Delta)$ computed for the RTM gather shown in Figure 6; the solid line is the best-fit parabola. (b) Dots – the squared traveltime $t^2\left(\left[X_1^\Delta\right]^2\right)$; solid – the best-fit straight line; the crosses mark the theoretical PS-wave hyperbolic moveout [equation (23)] with the NMO velocity computed using equation (28).

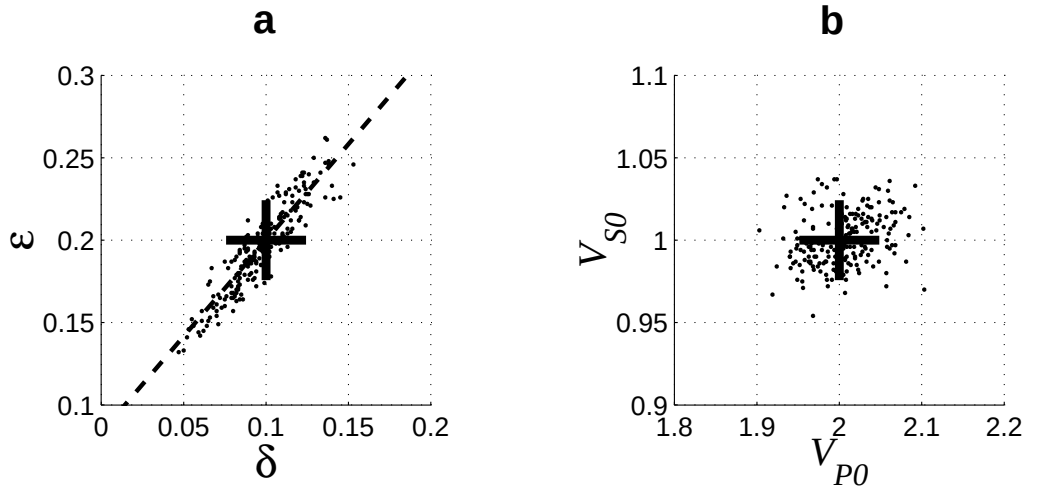

Figure 8. Anisotropic parameters ϵ and δ (a) and the vertical velocities V_{S0} and V_{P0} (b) determined by inverting P and PSV moveout data from a single dipping reflector. The input data were distorted by Gaussian noise with a standard deviation of 1% for the traveltimes and slownesses and 2% for the NMO velocities. Each dot represents the inversion result for a particular realization of the noise. The actual parameter values are marked by the crosses. The dashed line corresponds to the correct value of η. The correct reflector dip $\phi = 30°$.

tion (28)], where z in the reflector depth.

(iv) The slowness vectors $p_\ell^{\rm s}$, $p_\ell^{\rm r}$ and the PSV reflection traveltimes t^* at offsets $X^* = [-z/2,\ -z/4,\ 0,\ z/4,\ z/2]$.

The VTI parameters in Figure 8 were obtained for 200 realizations of noise-contaminated input data using least-squares minimization. Sufficient stability of the inversion procedure is confirmed by the relatively low standard deviations of V_{P0}, V_{S0}, ϵ and δ (2.0%, 1.6%, 0.03 and 0.02, respectively). The reflector depth z and the dip ϕ were estimated with the standard deviations 2.1% and 0.4°. Note that the values of ϵ and δ are scattered around the line corresponding to the correct value of η which is tightly constrained by the P-wave NMO ellipse.

The crucial pieces of information for the inversion were provided by the PSV-wave NMO velocities corresponding to the zero and nonzero initial offsets [items **(ii)** and **(iii)**]. It should be emphasized that excluding

any of those NMO velocities from the data reduces the stability of the inversion procedure.

PSH data

Since the P and PSV traveltimes already allowed us to estimate all relevant model parameters, the addition of PSH reflections might help to find Thomsen's coefficient γ and, therefore, fully characterize the VTI model. The well-known problem with PSH-data, however, is that there is no PSH-reflection in 2-D isotropic media and it is sometimes believed that this reflection event must always be weak and cannot provide reliable information about the medium parameters. The situation, however, becomes different in the presence of anisotropy where such reflections exist everywhere outside the vertical symmetry planes. The usefulness of PSH-type conversions for parameter estimation was demonstrated by Grechka, Theophanis and Tsvankin (1999) who showed how to obtain anisotropic coefficients of orthorhombic media using the split converted waves PS_1 and PS_2.

PSH-waves can also be observed in the higher-symmetry VTI media. As an example, Figure 9 shows the PSH-reflection computed in the two-layer VTI model from Figure 1. Clearly, the amplitude of the PSH-wave is comparable to that of the PSV-wave. Thus, the kinematics of the PSH-reflection can be used for parameter estimation. The amplitude of the PSH-wave can be further enhanced if we combine the seismograms recorded on in-line and cross-line components and properly rotate them.

Seismograms similar to that shown in Figure 9 indicate that the PSH-wave traveltimes are quite sensitive to the coefficient γ. Encouraged by this result, we supplemented the data used in the previous section by the NMO ellipse of the PSH-wave at zero offset ($X^* = 0$) and repeated the inversion. The inverted parameters from Figure 8 remained almost unchanged, while the coefficient γ was found with a standard deviation equal of 0.04.

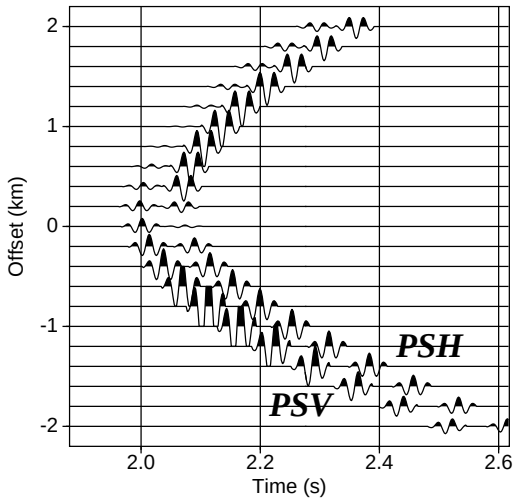

Figure 9. Horizontal in-line component of a ray-theoretical seismogram of the reflected PSV- and PSH-waves in the model from Figure 1. The values of Thomsen's coefficient γ in the layers are $\gamma_1 = \gamma_2 = 0.05$.

Discussion and conclusions

General results

Our work introduces a new approach to velocity analysis of converted waves. The key idea of our method is to resort PS-wave data into the so-called RTM gathers on which the reflection traveltime is symmetric in the vicinity of a chosen offset. This procedure enables one to apply conventional hyperbolic velocity analysis, originally developed for pure modes, to flatten the converted-wave moveout. The resorting into RTM gathers has the following attractive features:

(1) The information needed for the resorting includes only the slopes of the selected reflection event which can be measured on the common-shot and common-receiver sections. Knowledge of the model parameters is *not* required.

(2) RTM gathers can be built in the vicinity of any (not necessarily zero) source-receiver offset. This allows one to select for velocity analysis the portion of converted-wave data with the highest signal-to-noise ratio.

RTM gathers, however, have one important drawback stemming from the nature of the resorting procedure. Since the ratio of the source and receiver increments has to be found for each original offset and each reflection event separately, this ratio varies along a line and can be different for PS-waves reflected from different interfaces. Hence, the procedure of constructing RTM gathers has to be repeated many times which entails extensive computations.

Conventional velocity analysis applied to RTM gathers produces the PS-wave NMO velocity $V_{\mathrm{nmo},PS}$. Its azimuthal variation at zero offset has an oval shape which becomes elliptical only for a single homogeneous layer above a dipping reflector and for horizontally layered media. It is important to emphasize that the value of the NMO velocity $V_{\mathrm{nmo},PS}$ is influenced not only by the reflector dip and azimuth, but also by its curvature. Therefore, reflection point dispersal in incorporated into the PS-wave NMO velocity measured on RTM gather.

Parameter estimation

The converted-wave NMO velocity, similarly to the pure-mode NMO velocities, depends on the model parameters and, therefore, can be inverted for some of their combinations. Although it is not clear which parame-

ters are constrained for general anisotropy, we presented an example of successful parameter estimation for a homogeneous VTI layer using P-, PSV-, and PSH-wave traveltimes from a single dipping reflector. We were able to determine all layer parameters and reconstruct the model in the depth domain. Crucially important information for the inversion was provided by the azimuthally and offset-dependent PS-wave NMO velocities and by the NMO velocities corresponding to rays which propagate in directions different from those for zero-offset rays.

Acknowledgments

We are grateful to members of A(nisotropy)-team of the Center for Wave Phenomena (CWP), Colorado School of Mines, for helpful discussions. The support for this work was provided by the members of the Consortium Project on Seismic Inverse Methods for Complex Structures at CWP and by the United States Department of Energy (Award #DE-FG03-98ER14908).

References

Alkhalifah, T., and Tsvankin, I., 1995, Velocity analysis for transversely isotropic media: Geophysics, **60**, 1550–1566.

Granli, J.R., Arntsen, B., Sollid, A., and Hilde, E., 1999, Imaging through gas-filled sediments using marine shear-wave data: Geophysics, **64**, 668–667.

Grechka, V., Theophanis, S., and Tsvankin, I., 1999, Joint inversion of P- and PS-waves in orthorhombic media: Theory and a physical-modeling study: Geophysics, **64**, 146–161.

Grechka, V., and Tsvankin, I., 1998, 3-D description of normal moveout in anisotropic inhomogeneous media: Geophysics, **63**, 1079–1092.

Grechka, V. and Tsvankin, I., 1999, NMO-velocity surfaces and Dix-type formulae in heterogeneous anisotropic media: Geophysics, submitted.

Grechka, V., Tsvankin, I., and Cohen, J.K., 1999, Generalized Dix equation and analytic treatment of normal-moveout velocity for anisotropic media: Geophysical Prospecting, **47**, 117–148.

Sarkar, D., Lamb, B., and Castagna, J., 1999, AVO and velocity analysis: 69th Ann. Internat. Mtg., Soc. Expl. Geophys., Expanded Abstracts.

Thomsen, L., 1986, Weak elastic anisotropy: Geophysics, **51**, 1954–1966.

Thomsen, L., 1999, Converted-wave reflection seismology over inhomogeneous, anisotropic media: Geophysics, **64**, 678–690.

Tsvankin, I., and Grechka, V., 2000a, Dip moveout of converted waves and parameter estimation in transversely isotropic media: Geophysical Prospecting, **48**.

Tsvankin, I., and Grechka, V., 2000b, 3-D description of dip moveout of PS-waves and application to parameter estimation in VTI media: this volume.

Tsvankin, I., and Thomsen, L., 1994, Nonhyperbolic reflection moveout in anisotropic media: Geophysics, **59**, 1290–1304.

APPENDIX A: PS-wave NMO velocity in a homogeneous layer

Here we derive an expression for the PS-wave NMO velocity recorded at zero offset (i.e., $\mathbf{s}^* = \mathbf{r}^* \equiv \mathbf{y}^*$) over a single homogeneous anisotropic layer above a plane dipping reflector. We begin with rewriting the second-order traveltime derivatives $\dfrac{\partial^2 t}{\partial s_i\, \partial r_j}$ $(i,j=1,2)$ using the definitions (2) and (3) of the slowness vectors $\mathbf{p^r}$ and $\mathbf{p^s}$:

$$\frac{\partial^2 t(\mathbf{s},\mathbf{r})}{\partial s_i\, \partial r_j} = \frac{\partial p_i^{\mathbf{s}}}{\partial r_j} \tag{A1}$$

or

$$\frac{\partial^2 t(\mathbf{s},\mathbf{r})}{\partial s_i\, \partial r_j} = \frac{\partial p_j^{\mathbf{r}}}{\partial s_i}\,, \qquad (i,j=1,2)\,, \tag{A2}$$

where all derivatives are evaluated at $\mathbf{s} = \mathbf{r} = [y_1^*,\, y_2^*,\, 0]$.

In general, both the receiver coordinate $\mathbf{r}$ and the slowness $\mathbf{p^r}$ at the receiver can be treated as functions of the source position $\mathbf{s}$ and the slowness vector $\mathbf{p^s}$ at the source (or the shooting direction):

$$\mathbf{r} = \mathbf{r}\,(\mathbf{s},\, \mathbf{p^s}) \tag{A3}$$

and

$$\mathbf{p^r} = \mathbf{p^r}\,(\mathbf{s},\, \mathbf{p^s})\,. \tag{A4}$$

The last equation can be written explicitly because the slowness vector $\mathbf{p^r}$ is related to $\mathbf{p^s}$ by Snell's law

$$F \equiv (\mathbf{p^r} - \mathbf{p^s}) \times \mathbf{n} = 0\,, \tag{A5}$$

where $\mathbf{n}$ is the normal to the reflector. Since the reflector is plane and the layer is homogeneous, equation (A5) indicates that $\mathbf{p^r}$ does not depend on the source position $\mathbf{s}$. Thus, equation (A4) becomes

$$\mathbf{p^r} = \mathbf{p^r}\,(\mathbf{p^s})\,. \tag{A6}$$

This allows us to represent equations (A1) and (A2) in the following form:

$$\frac{\partial^2 t}{\partial s_i\, \partial r_j} = \frac{\partial p_i^{\mathbf{s}}}{\partial r_j} = \sum_{i'=1}^{2} \frac{\partial p_i^{\mathbf{s}}}{\partial p_{i'}^{\mathbf{r}}}\, \frac{\partial p_{i'}^{\mathbf{r}}}{\partial r_j} \tag{A7}$$

and

$$\frac{\partial^2 t}{\partial s_i\, \partial r_j} = \frac{\partial p_j^{\mathbf{r}}}{\partial s_i} = \sum_{j'=1}^{2} \frac{\partial p_j^{\mathbf{r}}}{\partial p_{j'}^{\mathbf{s}}}\, \frac{\partial p_{j'}^{\mathbf{s}}}{\partial s_i} \qquad (i,j=1,2)\,. \tag{A8}$$

Next, we will show that

$$\mathcal{D}_{ij} \equiv \frac{\partial p_i^{\mathbf{r}}}{\partial p_j^{\mathbf{s}}} \qquad (i,j=1,2) \tag{A9}$$

is simply the identity matrix, i.e,

$$\mathcal{D} = \begin{pmatrix} 1 & 0 \\ 0 & 1 \end{pmatrix}. \tag{A10}$$

To prove that, we differentiate equation (A5) with respect to $p_j^{\mathbf{s}}$ $(j=1,2)$. For $j=1$, we obtain

$$\frac{\partial F}{\partial p_1^{\mathbf{s}}} = \begin{pmatrix} \mathcal{D}_{12}\, n_3 - \left(q_{,1}^{\mathbf{r}}\, \mathcal{D}_{11} + q_{,2}^{\mathbf{r}}\, \mathcal{D}_{12} - q_{,1}^{\mathbf{s}}\right)\, n_2 \\ \left(q_{,1}^{\mathbf{r}}\, \mathcal{D}_{11} + q_{,2}^{\mathbf{r}}\, \mathcal{D}_{12} - q_{,1}^{\mathbf{s}}\right)\, n_1 - (\mathcal{D}_{11}-1)\, n_3 \\ (\mathcal{D}_{11}-1)\, n_2 - \mathcal{D}_{12}\, n_1 \end{pmatrix} = 0\,, \tag{A11}$$

where

$$q_{,i}^{\mathbf{r}} \equiv \frac{\partial p_3^{\mathbf{r}}}{\partial p_i^{\mathbf{r}}} \tag{A12}$$

and

$$q_{,i}^{\mathbf{s}} \equiv \frac{\partial p_3^{\mathbf{s}}}{\partial p_i^{\mathbf{s}}}\,, \qquad (i=1,2) \tag{A13}$$

denote the derivatives of the vertical slowness components with respect to the horizontal slownesses. Since the directions of the down- and up-going rays coincide (see Grechka, Tsvankin, and Cohen, 1999),

$$q_{,i}^{\mathbf{s}} = q_{,i}^{\mathbf{r}}\,. \tag{A14}$$

Also, the reflected ray cannot be parallel to the reflector, therefore,

$$n_1\, q_{,1}^{\mathbf{r}} + n_2\, q_{,2}^{\mathbf{r}} - n_3 \neq 0\,. \tag{A15}$$

Solving equations (A11) yields

$$\mathcal{D}_{11} = 1 \quad \text{and} \quad \mathcal{D}_{12} = 0\,. \tag{A16}$$

In a similar manner, differentiating equation (A5) with respect to $p_2^{\mathbf{s}}$, we obtain

$$\mathcal{D}_{21} = 0 \quad \text{and} \quad \mathcal{D}_{22} = 1\,, \tag{A17}$$

which proves equation (A10).

Thus, we can rewrite the derivatives (A7) and (A8) in the form

$$\frac{\partial^2 t}{\partial s_i\, \partial r_j} = \frac{\partial p_i^{\mathbf{r}}}{\partial r_j} = \frac{\partial p_j^{\mathbf{s}}}{\partial s_i} \tag{A18}$$

or, using the definitions (2) and (3) and expressions (26) and (27),

$$\frac{\partial^2 t}{\partial s_i\, \partial r_j} = \frac{U_{ij}^{\mathbf{r}}}{t^*} = \frac{U_{ij}^{\mathbf{s}}}{t^*} \qquad (i,j=1,2)\,. \tag{A19}$$

Finally, substituting this derivative into equation (28) for the PS-wave NMO velocity leads to

$$V_{\mathrm{nmo},PS}^{-2}(\alpha) = \boldsymbol{\ell}\, \mathbf{U}^{\mathbf{r}} \boldsymbol{\ell}^{\mathbf{T}} = \boldsymbol{\ell}\, \mathbf{U}^{\mathbf{s}} \boldsymbol{\ell}^{\mathbf{T}}\,, \tag{A20}$$

where the orientation of line $\boldsymbol{\ell}$ is given by equation (30),

$$\boldsymbol{\ell} = [\cos\alpha,\, \sin\alpha,\, 0]\,. \tag{A21}$$